Journal of Physics: Condensed Matter

PAPER

Leakage of Majorana mode into correlated quantum dot nearby its singlet-doublet crossover

To cite this article: T Zienkiewicz *et al* 2020 *J. Phys.: Condens. Matter* **32** 025302

IOP Publishing Journal of Physics: Condensed Matter
J. Phys.: Condens. Matter **32** (2020) 025302 (7pp) https://doi.org/10.1088/1361-648X/ab46d9

Leakage of Majorana mode into correlated quantum dot nearby its singlet-doublet crossover

T Zienkiewicz[1], J Barański[1], G Górski[2] and T Domański[3]

[1] Polish Air Force University, ul. Dywizjonu 303 no. 35, 08-521 Deblin, Poland
[2] Faculty of Mathematics and Natural Sciences, University of Rzeszów, 35-310 Rzeszów, Poland
[3] Institute of Physics, M. Curie-Skłodowska University, 20-031 Lublin, Poland

E-mail: j.baranski@law.mil.pl and doman@kft.umcs.lublin.pl

Received 4 July 2019, revised 5 September 2019
Accepted for publication 23 September 2019
Published 16 October 2019

Abstract
We study quasiparticle spectrum of the correlated quantum dot (QD) deposited on superconducting (SC) substrate which is side-coupled to the Rashba nanochain, hosting Majorana end modes. Ground state of an isolated QD proximitized to SC reservoirs is represented either by the singly occupied site or BCS-type superposition of the empty and doubly occupied configurations. Quantum phase transition between these distinct ground states is spectroscopically manifested by the in-gap Andreev states which cross each other at the Fermi level. This qualitatively affects leakage of the Majorana mode from the side-attached nanowire. We inspect the spin-selective relationship between the trivial Andreev states and the leaking Majorana mode, considering (i) perfectly polarized case, when tunneling of one spin component is completely prohibited, and (ii) another one when both spins are hybridized with the nanowire but with different couplings.

Keywords: quantum dots, Majorana quasiparticle, Andreev states

(Some figures may appear in colour only in the online journal)

1. Introduction

Recent development of the hybrid structures, comprising quantum dots (QDs) coupled the topologically superconducting (SC) nanowires [1–4] provide new challenges going beyond mere observation of the Majorana bound states (MBS). Since energy levels of QDs in such hybrid systems are experimentally tunable one can inspect interplay of the topological states with the correlation effects and proximity-induced electron pairing. Due to natural tendency of the Majorana modes to exist at boundaries of finite size systems, one may expect their leakage into any side-attached quantum dot (QD) [5] or more complex magnetic nanoislands [6].

It turns out, however, that efficiency of such process substantially depends on various parameters. For instance, in a weak coupling limit the Majorana modes show up either by the constructive or destructive interferometric line-shapes [7]. True leakage of Majorana mode into nontopological region is possible only in strongly hybridized structures [3, 8–11] as indeed reported experimentally [1–4]. But even under such conditions, leakage of the Majorana mode into the side-coupled QD region could be affected by additional effects, e.g. correlations. Influence of the Coulomb interactions (including the Kondo-regime) has been so far extensively studied, considering the QDs embedded between the normal or ferromagnetic leads [12–17]. Here we address another issue, studying competition between the Coulomb repulsion and electron pairing induced in the correlated QD proximitized to SC substrate. In particular, we focus on the role of quantum phase transition from the spinless (BCS-like) to the spinful (singly occupied) configurations. We analyze whether the Majorana mode would be able to leak into such configurations of the QD.

The paper is organized as follows. We present the physical situation of our interest (section 2) and introduce the relevant microscopic model (section 3). Next, we consider leakage of the Majorana mode into the QD for the fully (section 4) and partly polarized (section 5) cases. Finally, we summarize the results (section 6) and in appendix we give a brief reminder about the singlet-doubled transition in absence of the Majorana mode.

2. Physical setup

We consider the strongly correlated QD attached to the Rashba nanowire, both proximitized to the *s*-wave superconductor (SC). This setup (figure 1) could be realized in the scanning tunneling microscopy (STM) measurements, using Fe or Co nanoscopic chains on the SC Pb [18], Al or Re [4] substrates.

In realistic situations the spin–orbit coupling along with the Zeeman effect break spin-rotational symmetry of the system. Such nanowire brought in contact with superconductor develops the intersite pairing of parallel spins. They are 'tilted' with respect to *z*-axis, but one can project such pairing onto ↑ and ↓ components. For each of these sectors the intersite-pairing is characterized by effective amplitudes, mainly dependent on the applied magnetic field [19].

Upon entering the topological phase, there appear two Majorana quasiparticles simultaneously in both spin channels but with different spectral weights, what has been indeed reported in the STM measurements using a ferromagnetic tip [18]. Such issue has been recently addressed by several groups [11, 19, 20]. Klinovaja with co-workers [8] have shown that spin up and down tunneling amplitudes between MBSs and QD depend on the spin–orbit interaction length. Distance between the QD and topological nanowire determines oscillations of the tunneling amplitudes. By changing such dot-nanowire distance or varying the magnetic field one can thus tune the hybrid system either to the fully or to the partly polarized tunneling regimes.

For perfect spin polarization of the QD-chain tunneling (e.g. $t_\uparrow \neq 0,\ t_\downarrow = 0$) one would expect signatures of the zero-energy mode to appear only in one spin channel (for ↑ electrons). However, the proximity induced on-dot pairing between opposite spins mixes both these channels. Some aspects of this situation have been addressed in [7, 21, 22]. Since leakage of the Majorana (zero-energy) mode is sensitive to electronic states near the Fermi level, we would like to focus on crossing of the subg-gap (Andreev) states caused by competition between on-dot pairing and Coulomb repulsion (which is spectroscopically manifested by the singlet-doublet quantum phase transition). We show that signatures of the Majorana mode look completely different for both spin channels. In our considerations we take into account the case of (i) perfectly polarized tunneling of only one spin component while the other one is completely prohibited and (ii) another case where both spin electrons can be tunnel transferred, but with different amplitudes.

3. Microscopic model

To inspect the mutual relationship between the Majorana mode and in-gap features of the correlated QD we restrict our attention to the limit of large energy gap Δ of the SC reservoir. Under such conditions the single level QD is affected by the proximity-induced pairing. The proximitized QD is described by the Hamiltonian $\sum_\sigma \epsilon d^\dagger_\sigma d_\sigma + U n_\downarrow n_\uparrow + \frac{\Gamma_S}{2}(d_\uparrow d_\downarrow + d^\dagger_\downarrow d^\dagger_\uparrow)$, where local pairing is represented by the pair source/sink terms. We next consider its coupling to the Majorana zero mode (MZM) represented by $\sum_\sigma \lambda_\sigma \left(d^\dagger_\sigma \eta_1 + \eta_1 d_\sigma\right) + i\epsilon_m \eta_1\eta_2$. One can provide the following reasoning for the spin-dependent hybridization λ_σ of QD electrons with the Majorana mode. Because of the Rashba and Zeeman interactions (operating in the nanoscopic chains proximitized to SC substrates) the spin σ does no longer represent a *good quantum number* and the resulting intersite pairing is simultaneously driven in ↑ and ↓ sectors, although with different magnitudes mainly dependent on the magnetic field. For this reason the Majorana end-modes (induced via the Kitaev type mechanism) partly overlap with both spin electrons of the side-attached QD. More quantitative description of this issue has been presented by one of us (TD) in [19].

In our approach we recast the self-hermitian operators $\eta^\dagger_{1,2} = \eta_{1,2}$ by their standard fermionic equivalents [23] $\eta_1 = \frac{1}{\sqrt{2}}(f + f^\dagger)$ and $\eta_2 = \frac{-i}{\sqrt{2}}(f - f^\dagger)$. Effectively the low energy Hamiltonian can be expressed as

$$H^{\rm eff}_{\rm QD} \simeq \sum_\sigma \epsilon d^\dagger_\sigma d_\sigma + U n_\downarrow n_\uparrow + \frac{\Gamma_S}{2}(d_\uparrow d_\downarrow + d^\dagger_\downarrow d^\dagger_\uparrow) + \sum_\sigma t_{m\sigma}(d^\dagger_\sigma - d_\sigma)(f + f^\dagger) + \epsilon_m\left(f^\dagger f + \frac{1}{2}\right). \quad (1)$$

We assume that both spin components ($\sigma = \uparrow, \downarrow$) can be transferred between dot and Majorana host and $t_{m\sigma} = \lambda_\sigma/\sqrt{2}$ represent the hopping integrals of such processes.

Our objective is to determine the Green's functions $\mathcal{G}(\omega) = \langle\langle \Psi; \Psi^\dagger \rangle\rangle$ defined in the Nambu matrix notation $\Psi^\dagger = (d_\uparrow, d^\dagger_\uparrow, d_\downarrow, d^\dagger_\downarrow, f, f^\dagger)$. The equation of motion technique applied to noncorrelated problem yields

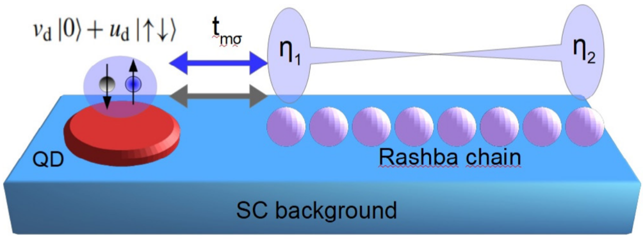

Figure 1. Schematic view of the correlated QD side-coupled to the Rashba nanowire and both deposited on SC substrate, where topological SC nanowire hosts two Majorana end-modes η_1 and η_2.

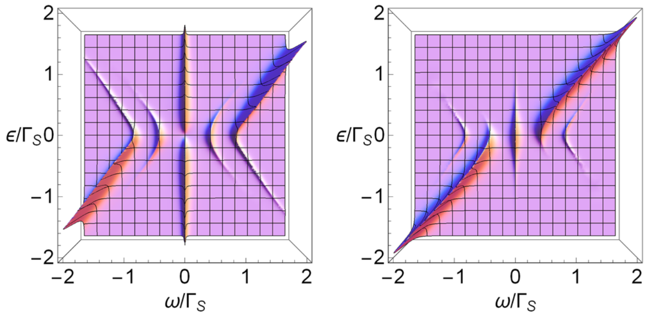

Figure 2. Density of states for spin ↑ (left) and ↓ (right) electrons obtained for $t_{m\uparrow} = 0.6\Gamma_S$, $t_{m\downarrow} = 0$ in absence of correlations ($U = 0$).

$$\lim_{U=0} \mathcal{G}^{-1}(\omega) = \begin{pmatrix} \omega-\epsilon+i\Gamma_N/2 & 0 & 0 & \Gamma_S/2 & -t_{m\uparrow} & -t_{m\uparrow} \\ 0 & \omega+\epsilon+i\Gamma_N/2 & -\Gamma_S/2 & 0 & t_{m\uparrow} & t_{m\uparrow} \\ 0 & -\Gamma_S/2 & \omega-\epsilon+i\Gamma_N/2 & 0 & -t_{m\downarrow} & -t_{m\downarrow} \\ \Gamma_S/2 & 0 & 0 & \omega+\epsilon+i\Gamma_N/2 & t_{m\downarrow} & t_{m\downarrow} \\ -t_{m\uparrow} & t_{m\uparrow} & -t_{m\downarrow} & t_{m\downarrow} & \omega-\epsilon_m & 0 \\ -t_{m\uparrow} & t_{m\uparrow} & -t_{m\downarrow} & t_{m\downarrow} & 0 & \omega+\epsilon_m \end{pmatrix}. \tag{2}$$

To account for the correlation effects one can numerically diagonalize 8×8 Hamiltonian matrix, determining the eigenenergies and transition elements between them. Another equivalent route can rely on the SC atomic limit solution [24], extending it to the present model

$$\mathcal{G}^{-1}(\omega) = \begin{pmatrix} G(\omega) & 0 & 0 & F(\omega) & 0 & 0 \\ 0 & -G^*(-\omega) & F^*(-\omega) & 0 & 0 & 0 \\ 0 & F^*(-\omega) & G(\omega) & 0 & 0 & 0 \\ F(\omega) & 0 & 0 & -G^*(-\omega) & 0 & 0 \\ 0 & 0 & 0 & 0 & \frac{1}{\omega-\epsilon_m} & 0 \\ 0 & 0 & 0 & 0 & 0 & \frac{1}{\omega+\epsilon_m} \end{pmatrix}^{-1} - \begin{pmatrix} 0 & 0 & 0 & 0 & t_{m\uparrow} & t_{m\uparrow} \\ 0 & 0 & 0 & 0 & -t_{m\uparrow} & -t_{m\uparrow} \\ 0 & 0 & 0 & 0 & t_{m\downarrow} & t_{m\downarrow} \\ 0 & 0 & 0 & 0 & -t_{m\downarrow} & -t_{m\downarrow} \\ t_{m\uparrow} & -t_{m\uparrow} & t_{m\downarrow} & -t_{m\downarrow} & 0 & 0 \\ t_{m\uparrow} & -t_{m\uparrow} & t_{m\downarrow} & -t_{m\downarrow} & 0 & 0 \end{pmatrix} \tag{3}$$

where

$$G(\omega) = \frac{\alpha_s\, u_d^2}{\omega - \left(\frac{U}{2}+E_d\right)} + \frac{\alpha_s\, v_d^2}{\omega + \left(\frac{U}{2}+E_d\right)} + \frac{\beta_s\, v_d^2}{\omega - \left(\frac{U}{2}-E_d\right)} + \frac{\beta_s\, u_d^2}{\omega + \left(\frac{U}{2}-E_d\right)}, \tag{4}$$

$$F(\omega) = \frac{\alpha_s\, u_d v_d}{\omega - \left(\frac{U}{2}+E_d\right)} - \frac{\alpha_s\, u_d v_d}{\omega + \left(\frac{U}{2}+E_d\right)} - \frac{\beta_s\, u_d v_d}{\omega - \left(\frac{U}{2}-E_d\right)} + \frac{\beta_s\, u_d v_d}{\omega + \left(\frac{U}{2}-E_d\right)}, \tag{5}$$

with the energy $E_d = \sqrt{(\epsilon + U/2)^2 + (\Gamma_S/2)^2}$, the usual BCS-type coefficients $u_d^2 = \frac{1}{2}\left[1 + \frac{\epsilon+U/2}{E_d}\right] = 1 - v_d^2$ and the relative spectral weights

$$\alpha_s = \frac{e^{\beta U/2} + e^{-\beta E_d}}{2e^{\beta U/2} + e^{-\beta E_d} + e^{\beta E_d}} = 1 - \beta_s. \tag{6}$$

In what follows we shall explore the quasiparticle spectrum of the correlated QD, assuming that the topological nanowire is long enough so that any overlap between the end-modes is negligible ($\epsilon_m \simeq 0$).

4. Fully polarized case

Let us first consider the fully spin-polarized case when tunneling of one spin component, say $\downarrow$, is totally prohibited. This situation could occur for very strong magnetic fields applied along the topological nanowire. We show that combined effect of MZM leakage and proximity induced pairing give rise to zero modes apparent in energy spectrum of both spin components even if tunneling rate of one spin is turned off. We inspect the influence of these zero states on the characteristic features of a phase transition from the BCS-like singlet state ($S = 0$) to the correlation-dominated doublet configuration. We show that even though zero modes appear in both spin channels, each of them have completely different character.

When a QD or other nanoobject is tunnel coupled to the Rashba chain hosting Majorana particles some part of these zero-energy modes can be transferred to QD region. In consequence, the spectral function of QD reveals additional feature pinned to the Fermi level. For the perfectly polarized tunneling amplitude ($t_{m\downarrow} = 0$ and $t_{m\uparrow} \neq 0$) one would expect such effect to modify only the spectral function of the directly coupled spin component [12, 13, 16, 17]. However, due to the SC proximity effect the electrons (say $\uparrow$) leaking from nanochain into QD region are bound into local pairs with their opposite spin ($\downarrow$) partners [7, 22]. Thereby, the Majorana mode becomes apparent in the energy spectrum of electrons for which the direct tunneling to nanochain is prohibited. This feature in $\downarrow$ spin sector, however, should be considered merely as a SC response for the leaking Majorana mode of the directly coupled spin $\uparrow$. Different nature of these zero-energy states is evident, both for the uncorrelated case (figure 2) and in a behavior of the Andreev states of the correlated QD near a quantum phase transition from the BCS-type singlet to the correlation driven doublet state (figure 3). These spectra are obtained at temperature $T = 0.1\Gamma_S$.

4.1. Energy spectrum of uncorrelated QD

Let us focus first on the noncorrelated case, $U = 0$. By inspecting the matrix Green's function (2) in the limit $\Gamma_N \to 0$ we notice that it is characterized by five poles: zero-energy state, two Andreev bound states at $\pm\sqrt{\epsilon^2 + (\Gamma_S/2)^2}$ and another two 'molecular' states $\pm\sqrt{\epsilon^2 + (\Gamma_S/2)^2 + (2t_{m\uparrow})^2}$, resulting from hybridization of the Andreev bound states with the Rashba chain [7]. In figure 2 we visualize qualitative differences between the spectral weights of $\uparrow$ and $\downarrow$ spin sectors obtained in the strong coupling limit $t_\uparrow = 0.6\Gamma_S$.

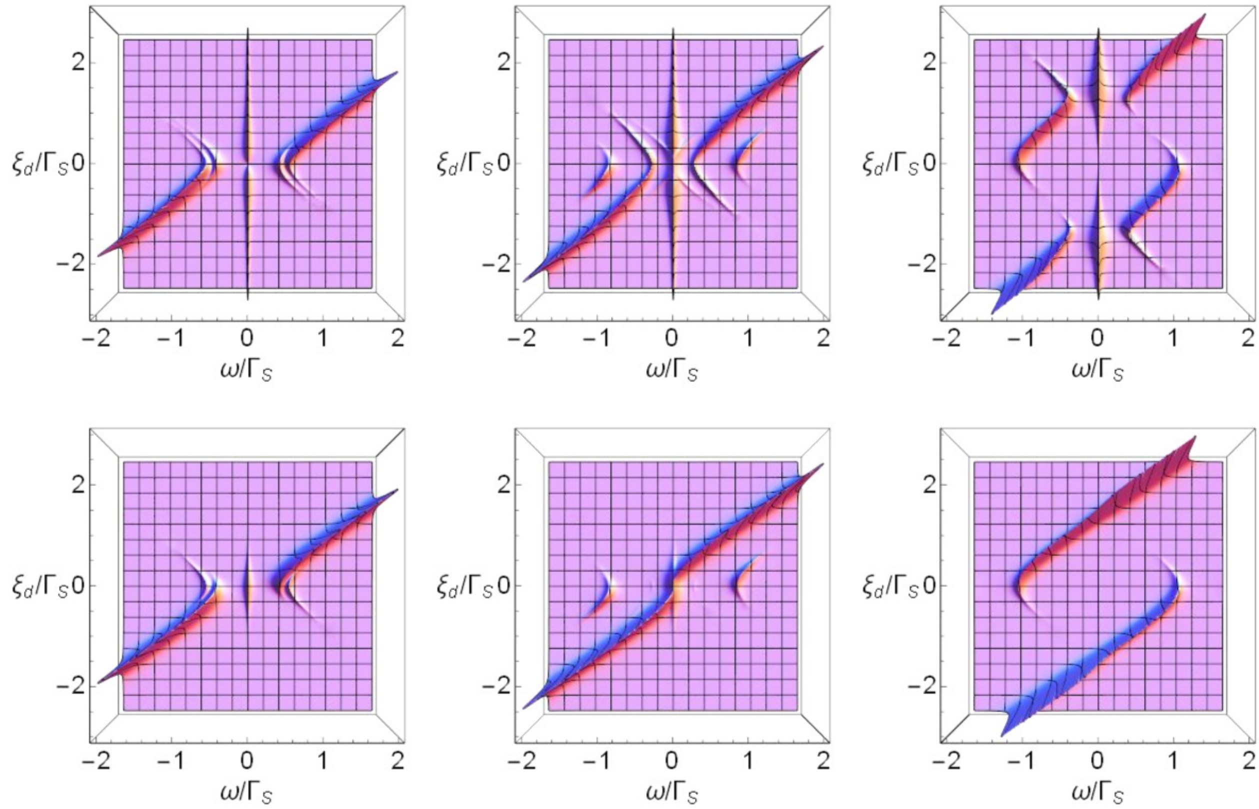

Figure 3. Density of states for spin ↑ (upper panel) and ↓ (bottom panel) electrons obtained for $t_{m\uparrow} = 0.3\Gamma_S$, $t_{m\downarrow} = 0$ and $U/\Gamma_S = 0$ (left panel), $U/\Gamma_S = 1$ (middle panel), $U/\Gamma_S = 3.5$ (right panel). Following [25] we denote by $\xi_d = \epsilon - U/2$.

In the spectrum of ↑ electrons we observe the well pronounced zero-energy mode directly leaking from the proximitized Rashba chain in much the same fashion as initially predicted for the QD attached to the Kitaev wire [5]. Contrary to that, the opposite spin electrons are not directly coupled to the chain therefore zero-energy mode emerges as a consequence of the local pairing. Some tiny Majorana mode shows up in this ↓ spin sector only when the QD energy ϵ is close to the Fermi level, otherwise it quickly fades away.

Furthermore, one can notice a small dip in the zero-energy signature of spin ↑ electrons appearing near $\epsilon = 0$. This comes from destructive feedback effect when the original QD level coincides with Majorana mode. Such destructive interference pattern has been described by our group [7, 22]. We have pointed out that even when spectral weight of the zero-energy mode in spectrum of directly coupled spins is suppressed, the zero-energy mode in opposite spin channel would be enhanced. As the QD-chain tunneling amplitude of spin ↓ electrons is turned off, spin ↓ electrons do not take part in destructive interference. Consequently in the left panel of figure 3 we observe well shaped zero mode. It is worth noticing that spectral weights of original Andreev states $(\pm\sqrt{\epsilon^2 + (\Gamma_S/2)^2})$ in spectrum of ↑ electrons are reduced in comparison with the molecular ones. Contrary to that, for electrons with prohibited dot-chain tunneling we observe that pure Andreev states are dominant.

4.2. Majorana near singlet-doublet crossover

We shall now discuss the correlation effects, driven by the Coulomb repulsion U. In absence of the Rashba nanowire upon varying the ratio U/Γ_S there appear the regular Andreev bound states at $\pm[U/2 - \sqrt{(\epsilon + U/2)^2 + (\Gamma_S/2)^2}]$ which eventually cross each other at the singlet-doublet (see appendix for an explanation of this quantum phase transition). Proximity induced zero-energy feature in the spin ↓ sector does not affect significantly this characteristic crossing, because it does not originate directly from the leaking Majorana mode. The strong Coulomb repulsion disfavors on-dot pairing, therefore upon increasing U/Γ_S also the side effects of the local pairing are gradually suppressed. One of them is the zero-energy mode appearing in the spectrum of spin ↓ electrons, originating solely from electron pairing. For this reason, upon traversing the singlet-doublet quantum phase transition the zero-energy mode of spin ↓ electrons is gradually washed out from the strongly correlated regime (see right bottom lower panel in figure 3).

In the case of spin ↑ electrons the spectrum looks completely different. Upon increasing the correlations strength the ABS states are split and form the molecular branches. These new states no longer cross each other. Approaching the singlet-doublet transition we observe emergence of the zero-energy state (directly leaking from the Rashba nanochain) while the

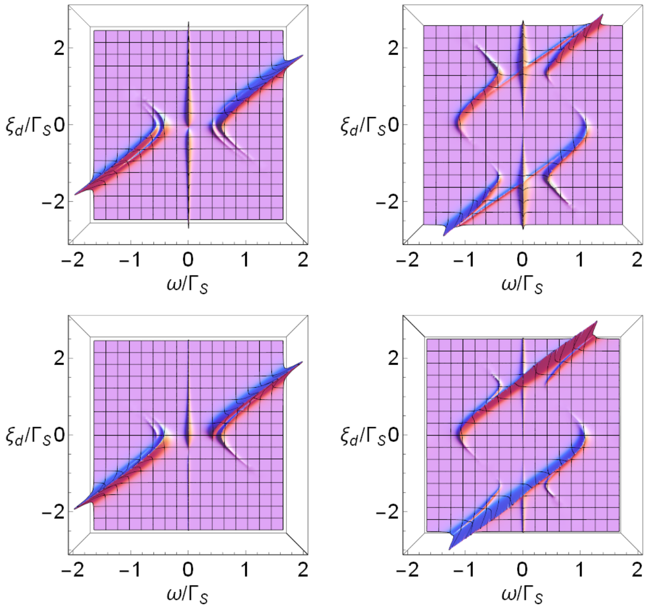

Figure 4. Density of states for spin up (upper panel) and spin down (bottom panel) electrons obtained for $t_{m\uparrow} = 0.3\Gamma_S, t_{m\downarrow} = 0.1\Gamma_S$ and $U/\Gamma_S = 0$ (left panel), $U/\Gamma_S = 3.5$ (right panel).

molecular Andreev states *repel* one another instead of the regular crossing (shown in figure A1). Such avoided-crossing behavior (see the upper right panel in figure 3) can be regarded as additional signature, of the proximity induced Majorana mode that repels the 'trivial' (finite-energy) Andreev states. This result generalizes the previously discussed topological/nontopological different nature of the bound states in hybrid structures comprising the uncorrelated QDs attached to the topological SC wires hosting the Majorana modes [3, 8–11]. We hope that empirical detection would be feasible using the spin-polarized STM measurements and varying the level ϵ of correlated QD by the gate potential.

5. Partial spin-polarization

Theoretical studies indicate that for specific conditions, it would be possible to achieve nearly perfectly spin polarized tunneling between the QD and chain [8]. However in realistic experimental setups both spin electrons can be transferred, although with substantially different tunneling amplitudes. In this subsection we briefly address such partially polarized case. Spin-resolved STM measurements [18] of the differential conductance obtained for Fe-atom chain deposited on the SC Pb-substrate using the ferromagnetic tip have revealed substantial magnetic polarization of the Majorana modes differing nearly 3-times between $\uparrow$ and $\downarrow$ components, respectively. Motivated by these empirical data, we assume in our approach the tunneling rate $t_{m\downarrow} = 0.1\Gamma_S$ being three times weaker than the coupling $t_{m\uparrow} = 0.3\Gamma_S$.

Figure 4 compares the density of states of each spin electrons in the non-correlated (left panels) and strongly correlated regime (right panels), respectively. In the strongly correlated limit we can practically observe a convolution of the features typical for each spin sectors of the fully polarized case. Yet one can clearly resolve the *avoided-crossing* behavior in the dominant $\uparrow$ spin coupling channel with the well pronounced Majorana mode separating them. Spectrum of the opposite spin sector, on the other hand, is predominantly reminiscent of the continuous Andreev band state branches with only very residual signatures of the zero-energy modes. Correlations could thus be very useful for distinguishing the qualitatively different character of the spin-polarized spectra of the QD.

6. Summary

We have studied the energy and spin-dependent spectra of the proximitized correlated QD attached to the topologically SC nanochain, hosting the Majorana end-modes. We have analyzed influence of the correlations (responsible for a quantum phase transition from the spinless BCS-type to the spinful configuration) on efficiency of the Majorana mode leakage. Our study predicts that the zero-energy states might appear in both spin sectors (due to the SC proximity effect), however their spectroscopic signatures are going to be qualitatively different. The spin channel which is directly coupled to the Majorana mode is characterized by (a) the well separated Andreev branches (of an avoided-crossing behavior) coexisting with (b) the zero-energy feature of a sizable spectral weight. The other spin sector, which is not directly coupled to the Majorana mode, in the strongly correlated limit is characterized by the continuous Andreev branches, traversing the zero energy without any trace of the leaking Majorana mode. Such spin sector can eventually allow the Majorana mode to appear but only in the weak correlation regime, when the proximitized QD stays in the BCS-type configuration.

Correlations can hence be very beneficial for the spin-selective leakage of the Majorona modes onto the correlated QDs. Such effects would be detectable, e.g. using the polarized STM measurement analogous to those already reported in [18]. Another interesting realization of unique features of the leaking Majorana mode near the singlet-doublet quantum phase transition could be possible when the correlated QD is sandwiched between two SC leads. In such geometry the Majorana is expected to induce $0-\pi$ transition [26–29], and this in turn would be easily observable by the reversal of d.c. Josephson current.

Acknowledgments

This research has been conducted in the framework of the project 'Analysis of nanoscopic systems coupled to superconductors in the context of quantum information processing' No. GB/5/2018/209/2018/DA funded in period 2018–2021 by the Ministry of National Defense Republic of Poland (JB, TZ). This project has been also supported by National Science Centre (NCN, Poland) under the Grants UMO-2018/29/B/ST3/00937 (GG) and UMO-2017/27/B/ST3/01911 (TD).

Appendix. Quantum phase transition in absence of Majorana mode

For illustration of the singlet-doublet phase transition let us briefly recall the results for the proximitized and correlated QD in absence of the Rashba chain. To determine the trivial Andreev states in presence of the correlation effects we focus on the exact solution in the SC atomic limit, when the proximitized QD is described by the Hamiltonian [30]

$$H_{\mathrm{QD}}^{\mathrm{prox}} = \sum_{\sigma} \epsilon d_{\sigma}^{\dagger} d_{\sigma} + U n_{\downarrow} n_{\uparrow} + \left(\Delta d_{\downarrow}^{\dagger} d_{\uparrow}^{\dagger} + \mathrm{h.c.} \right) \tag{A.1}$$

with the pairing potential $\Delta = \Gamma_S/2$. The eigenstates of this simple problem (A.1) are represented either by the spinful configurations $|\sigma\rangle$ with eigenenergy ϵ, or the spinless (BCS-type) states [25, 31]

$$|\mathrm{BCS}_{-}\rangle = u_d|0\rangle - v_d|\uparrow\downarrow\rangle, \tag{A.2}$$

$$|\mathrm{BCS}_{+}\rangle = v_d|0\rangle + u_d|\uparrow\downarrow\rangle \tag{A.3}$$

with eigenenergies

$$E_{\mp} = \left(\epsilon + \frac{U}{2}\right) \mp \sqrt{\left(\epsilon + \frac{U}{2}\right)^2 + \Delta^2} \tag{A.4}$$

and the diagonalizing coefficients

$$u_d^2, v_d^2 = \frac{1}{2}\left[1 \pm \frac{\epsilon + U/2}{\sqrt{(\epsilon + U/2)^2 + \Delta^2}}\right]. \tag{A.5}$$

Using the spectral Lehmann representation we can apply these eigenvectors $|j\rangle$ and eigenvalues E_j to construct the Fourier transforms of the retarded Green's functions

$$\langle\langle A; B\rangle\rangle_{\omega} = \frac{1}{\mathcal{Z}} \sum_{i,j} \frac{\mathrm{e}^{-\beta E_i} + \mathrm{e}^{-\beta E_j}}{\omega + E_i - E_j} \langle j|A|i\rangle \, \langle i|B|j\rangle \tag{A.6}$$

with the partition function $\mathcal{Z} = \sum_{j=1}^{4} \mathrm{e}^{-\beta E_j}$ and inverse temperature $\beta = (k_{\mathrm{B}}T)^{-1}$. Since in our case the particle and hole degrees of freedom are mixed with one another (via pairing terms) we need both, the normal $G(\omega) = \langle\langle d_{\uparrow}; d_{\uparrow}^{\dagger}\rangle\rangle_{\omega+i0^+}$ and the anomalous $F(\omega) = \langle\langle d_{\uparrow}; d_{\downarrow}\rangle\rangle_{\omega+i0^+}$ propagators. Computing the matrix elements for the creation and annihilation operators $\langle i|d_{\sigma}^{(\dagger)}|j\rangle$ we finally obtain the Green's functions presented in equations (4) and (5). The effective quasiparticle excitations (in absence of the Majorana mode) can be inferred from the (normal) spectral function $\rho(\omega) = -\frac{1}{\pi}\mathrm{Im}G(\omega + i0^+)$ which for representative values of the Coulomb potential is displayed in figure A1. In general we can notice four branches of the quasiparticle excitation at energies $\pm U/2 \pm \sqrt{(\epsilon + U/2)^2 + \Delta^2}$. Two of them $\pm\left(U/2 - \sqrt{(\epsilon + U/2)^2 + \Delta^2}\right)$ can be regarded as the low-energy excitations, while the other ones (shifted from them by U) represent the high-energy features that in realistic systems are usually pushed to a continuum existing outside the subgap regime (because U is typically much larger than Δ).

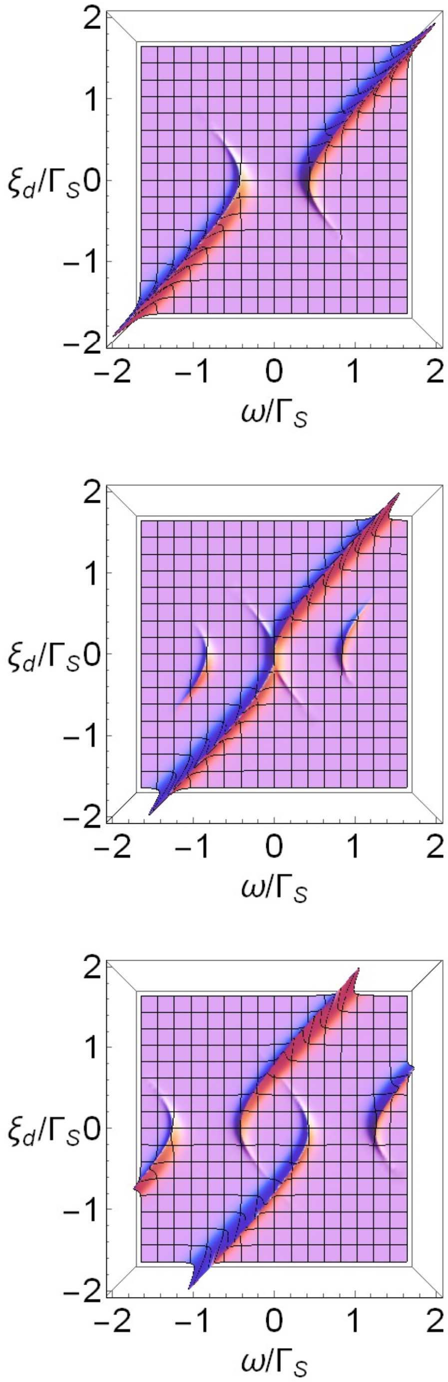

Figure A1. Spectral function $\rho(\omega)$ of the correlated QD as a function of the energy $\xi_d = \epsilon + U/2$ obtained at low temperature $T = 0.1\Gamma_S$ in the 'superconducting atomic limit' $\Gamma_N \to 0^+$ for $U = 0$ (upper panel) $U = \Gamma_S$ (middle panel), $U = 2\Gamma_S$ (bottom panel).

Additionally, we can also use the off-diagonal spectral function $\rho_{\mathrm{off}}(\omega) = -\frac{1}{\pi}\mathrm{Im}F(\omega + i0^+)$ which brings information about the induced order parameter $\langle d_{\downarrow} d_{\uparrow}\rangle = \int_{-\infty}^{\infty} \mathrm{d}\omega \rho_{\mathrm{off}}(\omega) \left[1 + \mathrm{e}^{\beta\omega}\right]^{-1}$. In particular it has been shown [25], that crossings of the Andreev quasiparticle coincide with abrupt changes, both of the magnitude and sign of $\langle d_{\downarrow} d_{\uparrow}\rangle$ (hence the name '$0 - \pi$' transition). For the weak correlation limit $U < \Gamma_S$ the ground state is represented by the singlet configuration in entire range of the QD level ϵ. In such case, the density of states consists of only two Andreev bound states branches separated by the pairing gap (figure A1). For stronger correlations U, these subgap branches approach each other and they eventually cross at the singlet-doublet phase boundaries. The critical interaction corresponding to such transition at the half filling is $U = \Gamma_S$ (see the middle panel in figure A1). In the doublet regime ($U > \Gamma_S$), the subgap Andreev branches always cross each other at some energy ϵ (bottom panel in figure A1). The border line of such singlet-doublet (or $0 - \pi$) transition is thus dependent on the Coulomb potential U and the QD level ϵ [25].

In presence of the Majorana mode (in section 4) we noticed, that the states appearing in spin $\downarrow$ electron spectrum exhibit similar behavior (see bottom panels in figure 3). Presence of the zero-energy state in this spin channel did not affect significantly the characteristics of the singlet-doublet transition. In contrast, for spins directly coupled to nanochain, we note the qualitatively different *avoided-crossing* behavior.

ORCID iDs

J Barański https://orcid.org/0000-0002-0963-497X
T Domański https://orcid.org/0000-0003-1977-3989

References

[1] Deng M T, Vaitiekenas S, Hansen E B, Danon J, Leijnse M, Flensberg K, Nygård J, Krogstrup P and Marcus C M 2016 Majorana bound state in a coupled quantum-dot hybrid-nanowire system *Science* **354** 1557
[2] Nichele F *et al* 2017 Scaling of Majorana zero-bias conductance peaks *Phys. Rev. Lett.* **119** 136803
[3] Deng M-T, Vaitiekėnas S, Prada E, San-Jose P, Nygård J, Krogstrup P, Aguado R and Marcus C M 2018 Nonlocality of Majorana modes in hybrid nanowires *Phys. Rev.* B **98** 085125
[4] Kim H, Palacio-Morales A, Posske T, Rózsa L, Palotás K, Szunyogh L, Thorwart M and Wiesendanger R 2018 Toward tailoring Majorana bound states in artificially constructed magnetic atom chains on elemental superconductors *Sci. Adv.* **4** eaar5251
[5] Vernek E, Penteado P H, Seridonio A C and Egues J C 2014 Subtle leakage of a Majorana mode into a quantum dot *Phys. Rev.* B **89** 165314
[6] Mascot E, Cocklin S, Rachel S and Morr D K 2018 Quantum engineering of Majorana fermions *in preparation* (arXiv:1811.06664)
[7] Górski G, Barański J, Weymann I and Domański T 2018 Interplay between correlations and Majorana mode in proximitized quantum dot *Sci. Rep.* **8** 15717
[8] Hoffman S, Chevallier D, Loss D and Klinovaja J 2017 Spin-dependent coupling between quantum dots and topological quantum wires *Phys. Rev.* B **96** 045440
[9] Prada E, Aguado R and San-Jose P 2017 Measuring Majorana nonlocality and spin structure with a quantum dot *Phys. Rev.* B **96** 085418
[10] Ptok A, Kobiałka A and Domański T 2017 Controlling the bound states in a quantum-dot hybrid nanowire *Phys. Rev.* B **96** 195430
[11] Szumniak P, Chevallier D, Loss D and Klinovaja J 2017 Spin and charge signatures of topological superconductivity in Rashba nanowires *Phys. Rev.* B **96** 041401
[12] Lee M, Lim J S and López R 2013 Kondo effect in a quantum dot side-coupled to a topological superconductor *Phys. Rev.* B **87** 241402
[13] López R, Lee M, Serra L and Lim J S 2014 Thermoelectrical detection of Majorana states *Phys. Rev.* B **89** 205418
[14] Ruiz-Tijerina D A, Vernek E, Dias da Silva L G G V and Egues J C 2015 Interaction effects on a majorana zero mode leaking into a quantum dot *Phys. Rev.* B **91** 115435
[15] Silva J F and Vernek E 2016 Andreev and Majorana bound states in single and double quantum dot structures *J. Phys.: Condens. Matter* **28** 435702
[16] Weymann I 2017 Spin Seebeck effect in quantum dot side-coupled to topological superconductor *J. Phys.: Condens. Matter* **29** 095301
[17] Weymann I and Wójcik K P 2017 Transport properties of a hybrid Majorana wire-quantum dot system with ferromagnetic contacts *Phys. Rev.* B **95** 155427
[18] Jeon S, Xie Y, Li J, Wang Z, Bernevig B A and Yazdani A 2017 Distinguishing a Majorana zero mode using spin-resolved measurements *Science* **358** 772
[19] Maśka M and Domański T 2017 Polarization of the Majorana quasiparticles in the Rashba chain *Sci. Rep.* **7** 16193
[20] Li J, Jeon S, Xie Y, Yazdani A and Bernevig B A 2018 Majorana spin in magnetic atomic chain systems *Phys. Rev.* B **97** 125119
[21] Chirla R and Moca C P 2016 Fingerprints of Majorana fermions in spin-resolved subgap spectroscopy *Phys. Rev.* B **94** 045405
[22] Barański J, Kobiałka A and Domański T 2017 Spin-sensitive interference due to Majorana state on the interface between normal and superconducting leads *J. Phys.: Condens. Matter* **29** 075603
[23] Elliott S R and Franz M 2015 Colloquium: Majorana fermions in nuclear, particle, and solid-state physics *Rev. Mod. Phys.* **87** 137
[24] Vecino E, Martín-Rodero A and Levy Yeyati A 2003 Josephson current through a correlated quantum level: Andreev states and π junction behavior *Phys. Rev.* B **68** 035105
[25] Bauer J, Oguri A and Hewson A C 2007 Spectral properties of locally correlated electrons in a Bardeen–Cooper–Schrieffer superconductor *J. Phys.: Condens. Matter* **19** 486211
[26] Awoga O, Cayao J and Black-Schaffer A 2019 Supercurrent detection of topologically trivial zero-energy states in nanowire junctions *Phys. Rev. Lett.* **123** 117001
[27] Cayao J, Black-Schaffer A, Prada E and Aguado R 2018 Andreev spectrum and supercurrents in nanowire-based SNS junctions containing Majorana bound states *Beilstein J. Nanotechnol.* **9** 1339
[28] Cayao J, San-Jose P, Black-Schaffer A, Aguado R and Prada E 2017 Majorana splitting from critical currents in Josephson junctions *Phys. Rev.* B **96** 205425
[29] Cayao J, Prada E, San-Jose P and Aguado R 2015 SNS junctions in nanowires with spin–orbit coupling: role of confinement and helicity on the subgap spectrum *Phys. Rev.* B **91** 024514
[30] Martín-Rodero A and Levy Yeyati A 2012 The Andreev states of a superconducting quantum dot: mean field versus exact numerical results *J. Phys.: Condens. Matter* **24** 385303
[31] Barański J and Domański T 2013 In-gap states of a quantum dot coupled between a normal and a superconducting lead *J. Phys.: Condens. Matter* **25** 435305